FULL PAPER

Dalton
www.rsc.org/dalton

Evidence for chiral discrimination of ruthenium(II) polypyridyl complexes by DNA †

Paul P. Pellegrini and Janice R. Aldrich-Wright *
College of Science Technology and Environment, School of Science, Food and Horticulture, University of Western Sydney, Penrith South, NSW, Australia.
E-mail: J.Aldrich-Wright@uws.edu.au

Received 28th August 2002, Accepted 13th November 2002
First published as an Advance Article on the web 10th December 2002

Here we report on the synthesis and enantiomeric resolution of metal complexes of the type $[Ru(bpyMe_2)_2L]^{2+}$ (where $bpyMe_2$ = 4,4′-dimethyl-2,2′-bipyridine and L = 1,10-phenanthroline (phen), dipyrido[3,2-*a*:2′3′-*c*]-quinoxaline (dpq), dipyrido[3,2-*a*:2′3′-*c*](6,7,8,9-tetrahydro)phenazine (dpqc) or dipyrido[3,2-*a*:2′3′-*c*]phenazine (dppz)). DNA-paper chromatography, absorption spectroscopy, gel electrophoresis and viscometry of linear DNA were used to assess the association and affinity for DNA of the aforementioned complexes. Optical resolution of the complexes was achieved by solvent recycled chromatography using Sephadex cation exchange resin and disodium (−)-*O*,*O*′-dibenzoyl-L-tartrate. Paper chromatography successfully elucidated the relative binding affinities of the metal complexes investigated in the following order phen (0.68) < dpq (0.36) < dpqc (0.14) < dppz (0.09). Absorption spectroscopy experiments indicated that each of the complexes were in close association with the DNA. Electrophoresis of the plasmid DNA incubated with the Δ complexes of dppz or dpqc show unwinding. The Λ-isomer of dppz resulted in smearing due to less effective binding whereas the Λ-isomer of dpqc showed no unwinding at all. Unexpectedly, *rac*-$[Ru(bpyMe_2)_2(dpq)]^{2+}$ showed greater unwinding than either isomer. DNA-viscosity experiments provided evidence that both the Δ and Λ-isomers of dppz and dpqc bind by intercalation. However, Δ and Λ-$[Ru(bpyMe_2)_2(dpq)]^{2+}$ bind through different modes, the Δ isomer by intercalation and the Λ isomer by partial intercalation. The conclusions that can be drawn from this is that the extended methyl groups in the 4- and 4′-positions on the $bpyMe_2$ ligand are critical in eliciting different enantiomeric interactions with the walls of the DNA grooves.

Introduction

The interaction of DNA with inert octahedral metal complexes has been a vibrant area of research for some time.[1–15] Despite a significant amount of research published to date, our understanding of the nature of the binding geometries of these complexes to DNA is still limited. In the elucidation of the reversible reactions of DNA, Ru(II)–polypyridyl complexes have proven invaluable as they are easily synthesised, resolvable and stable in their enantiomeric forms, thus providing sturdy complexes with which to investigate DNA.

Constructing these molecules has for the most part looked at intercalation potential by incorporating larger or suitably shaped ligands for coordination to create complexes such as $[Ru(ancillary)_2(intercalator)]^{2+}$ where ancillary has mostly included 1,10-phenanthroline (phen) or 2,2′-bipyridine (bpy) and intercalator has been phen,[1–8] dipyrido[3,2-*a*:2′3′-*c*]quinoxaline (dpq),[9–11] dipyrido[3,2-*a*:2′3′-*c*](6,7,8,9-tetrahydro)-phenazine (dpqc),[10] dipyrido[3,2-*a*:2′3′-*c*]phenazine (dppz)[12–15] (Fig. 1). The objective has been to explore the combination of various intercalator and ancillary ligand types[9–11,15] to modulate the interaction between the complex and DNA and to accentuate any enantiomeric differences.

As controversy still surrounds the binding of $[Ru(phen)_3]^{2+}$ to nucleic acids, including complexes that contain phen was seen to be a vital inclusion in this study as they represent the weakest binding moieties thought to be capable of intercalating. At the other end of the spectrum, the dppz ligand[9–11,15,16] will be employed to provide complexes with much higher binding affinities for DNA. However, when incorporated into complexes, dppz has proven itself to be a moiety that intercalates without site selectivity. In between phen and dppz, in terms of overall intercalator size, are the ligands dpq[9–11,17] and dpqc.[10,18]

Having discussed the ligands intended for intercalation into DNA, it is important to mention the peripheral ligands and the desired influences that they will bring about as a result of their association with DNA. The bidentate 4,4′-dimethyl-2,2′-bipyridine ($bpyMe_2$) was chosen because computer generated intercalation models of the metal complex $[Ru(bpyMe_2)_2(intercalator)]^{2+}$ with two base-pairs, indicate that only the intercalator has any potential aromatic overlap. The extended methyl groups are expected to interacted with the walls of the groove with some enantioselectivity in much the same way that $[Ru(DIP)_3]^{2+}$ [19] does, albeit to a lesser extent.

DNA bound cellulose paper chromatography is a straightforward method for studying interactions of compounds with DNA.[20] This technique tests the relative affinity of a drug for DNA, and while it does not discern between binding modes the affinity may be indicative of it.

Owing to the strong MLCT bands of polypyridyl–Ru(II) complexes, the high molar extinction coefficients lend themselves to absorption analysis upon binding to DNA. When associating with DNA, the visible electronic absorption of the complexes is changed, and the hypochromic or hyperchromic effects at the band maxima can be indicative of an association.[21–23] A suggested explanation for this is the strong interaction between the DNA bases and the intercalating chromophore.[1,24] It has been argued that this particular type of absorption spectroscopy alone cannot possibly deduce whether a species intercalates or surface binds.[25]

For DNA to accommodate the physical strain of intercalation unwinding of the double helix is necessary. Submarine gel electrophoresis and viscometry are techniques that identify this effect upon binding. Unwinding of DNA by established intercalators such as ethidium[26] as well as for $[Ru(phen)_3]^{2+}$,[1,4] has been reported. It is unlikely that submarine gel electrophoresis can discriminate between classical and partial intercalation, as both binding modes require unwinding. Apart from the determination of unwinding angles by using Topoisomerase

† Electronic supplementary information (ESI) available: absorption spectra. See http://www.rsc.org/suppdata/dt/b2/b208147d/

DOI: 10.1039/b208147d

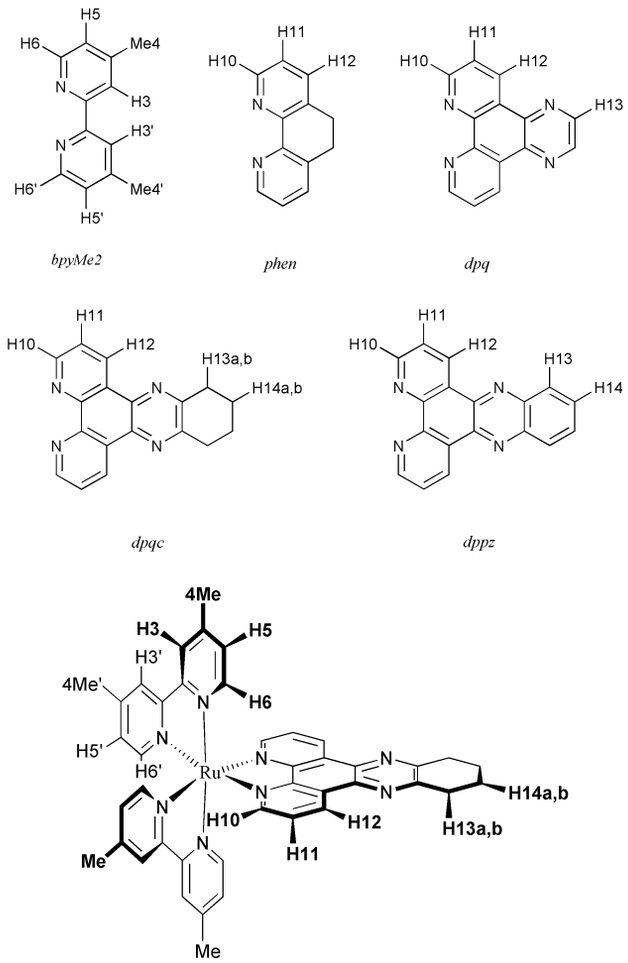

Fig. 1 Structure and atom numbering of the ligands $bpyMe_2$, phen, dpq, dpqc and dppz and the proton assignments of $[Ru(bpyMe_2)_2(dpqc)]^{2+}$. Note the greater proximity that the H3, 4Me, H5 and H6 protons have with the dpqc's H10, H11 and H12 than the H3′, 4Me′, H5′ and H6′ protons, respectively. It is this property that is responsible for the differing resonances of the corresponding protons.

I enzymes,[4,26–28] gel electrophoresis has been used successfully for DNA cleavage experiments, even for Ru(II) complexes such as $[Ru(bpy)_3]^{2+}$ and $[Ru(phen)_3]^{2+}$.[29,30] The measurement of viscosity is an efficient and straightforward means of determining whether a compound intercalates into DNA. According to the classical intercalation concept put forward by Lerman,[31] when a drug intercalates between the base-pairs of DNA, its presence forces these base-pairs away from each other and therefore unwinds the double helix and lengthens a given amount of DNA. This in turn increases the viscosity of the solution. The calf thymus (CT-DNA) must be linear in order for the measurements to be made, so it is cleaved to short rod-like lengths too small for the tertiary structure to predominate (usually about 200 bp). This technique is very sensitive to the changes in DNA length because viscosity is proportional to L^3 (where L is the length of linear DNA).[32–34]

Herein we describe the synthesis, resolution and characterisation of the metal complexes of the type Δ,Λ-$[Ru(bpyMe_2)_2(intercalator)]^{2+}$ (intercalator is phen, dpq, dpqc or dppz) as well as their effects on DNA by the techniques of DNA-paper chromatography, absorption spectroscopy, electrophoresis, and viscosity measurements for any enantioselectivity.

Experimental

Materials

1,10-Phenanthroline, 4,4′-dimethyl-2,2′-bipyridine, ruthenium trichloride hydrate, lithium chloride, potassium hexafluorophosphate, sodium acetate, sodium phosphate dibasic, sodium phosphate monobasic, sodium chloride, sodium hydroxide, sodium borohydride, sodium periodate, ethidium bromide, Hoechst33258, tris(hydroxymethyl)aminomethane, tris(hydroxymethyl)aminomethane hydrochloride, aluminium oxide (neutral Brockmann I), ethylenediaminetetraacetic acid, and Amberlite IRA 400(Cl), SP Sephadex C-25 ion exchange resins were all obtained from the Aldrich Chemical Company, Inc., USA. Dibenzoyl-L-tartaric acid monohydrate was purchased from Fluka A.G. Calf-thymus DNA (Type I highly polymerised sodium salt form) and pBR322 plasmid DNA were purchased from the Sigma Chemical Company.

Instrumentation

Electronic absorption spectra were recorded on a Cary 1E spectrophotometer (quartz cell length was 1 cm). ESI mass spectra were recorded on a VG-Quattro mass spectrometer at 50 eV and alternating positive and negative collection modes. Circular dichroism spectra were recorded on a JASCO 500C spectropolarimeter. Proton NMR was obtained using a Varian 300 MHz spectrometer.

Synthesis

Synthesis of intercalating ligands. The bidentate ligands dpq,[9–11,17] dpqc[10,18] and dppz[16] were all synthesised according to published methods. The synthetic routes all proceeded *via* 1,10-phenanthroline-5,6-dione produced by the oxidation of 1,10-phenanthroline using the method of Yamada and co-workers.[35] Subsequent condensation of this species with the required diamine in alcohol produced the desired ligand in reasonable yields.

Syntheses and resolution of Δ,Λ-$[Ru(bpyMe_2)_2L](PF_6)_2\cdot xH_2O$, where L = phen, dpq, dpqc or dppz. A mixture of $[Ru(bpyMe_2)_2Cl_2]\cdot 3H_2O$[36] (175 mmol) and L (200 mmol) was stirred under reflux for 3 h in a de-aerated 1:1 ethanol–water solution (400 cm^3). The resulting deep red solution was evaporated under reduced pressure until all of the ethanol was distilled off. The excess ligand was filtered off and a saturated aqueous solution of sodium hexafluorophosphate (2 cm^3) was added dropwise to the stirred filtrate. The resulting orange–red solid was filtered off, washed with cold water (3 × 10 cm^3), diethyl ether (3 × 10 cm^3) and then dried under suction. This crude product was recrystallised from a 1:2 water–acetone solution or alternatively, could be dissolved in the minimum amount of acetonitrile and chromatographed on a column of aluminium oxide (neutral Brockmann I) with acetonitrile as the eluent. The major red band was collected and the complex was precipitated and dried.

The enantiomers of $[Ru(bpyMe_2)_2L](PF_6)_2\cdot xH_2O$ (where L = phen, dpq, dpqc or dppz) were resolved using solvent-recycled chromatography[37] on a Sephadex SP-C25 column (100 × 1.6 cm) utilising 0.1 M disodium-*O,O′*-dibenzoyl-L-tartrate (and 5% acetone, only with the dppz complex). The effective column length was 0.9, 1.2, 1.2 and 1.4 m for the complexes containing phen, dpq, dpqc and dppz, respectively. The enantiomeric purity of the chloride salt was determined by circular dichroism spectroscopy and the relative absorbance at 456 nm.

$[Ru(bpyMe_2)_2(phen)](PF_6)_2\cdot 2H_2O$:[38] 79%. λ_{max}/nm (ε/dm^3 mol^{-1} cm^{-1}) (water–acetone): 456 (14100). MS (ESMS, CH_3CN, M = 941.7); m/z = 795.0 $(M-PF_6)^+$. CD: λ/nm ($\Delta\varepsilon$/dm^3 mol^{-1} cm^{-1}) (ethanol–water): Δ isomer: 400 (+63); 465 (−64.2); Λ isomer: 400 (−72.4); 457 (+69.3). Optical purity at 465 nm = 92.6%.[39]

$[Ru(bpyMe_2)_2(dpq)](PF_6)_2\cdot 2H_2O$: 79%. λ_{max}/nm (ε/dm^3 mol^{-1} cm^{-1}) (water–acetone): 439 (13900). δ_H (300 MHz, CD_3CN): 9.34 (H13; 2H, s), 9.61 (H12; 2H, d, J = 5.4 Hz), 8.06 (H11, 2H, dd, J = 8.3, 5.4 Hz), 8.74 (H3′; 2H, s), 8.68 (H3; 2H, s), 8.54 (H10; 2H, d, J = 8.3 Hz), 7.96 (H6′; 2H, d, J = 5.4 Hz), 7.78

(H6, 2H, d, J = 5.4 Hz), 7.44 (H5′; 2H, d, J = 5.4 Hz), 7.18 (H5, 2H, d, J = 5.4 Hz), 2.62 (4Me′; s, 6H), 2.51 (4Me; s, 6H). MS (ESMS, CH_3CN, M = 993.7); m/z = 846.9 $(M - PF_6)^+$. CD: λ/nm ($\Delta\varepsilon$/dm^3 mol^{-1} cm^{-1}) (ethanol–water): Δ isomer: 415 (+52.4); 476 (−37.9); Λ isomer: 415 (−52.2); 476 (+38.6). Optical purity at 476 nm = 98.1%.[39]

$[Ru(bpyMe_2)_2(dpqc)](PF_6)_2 \cdot 2H_2O$: 82%. λ_{max}/nm (ε/dm^3 mol^{-1} cm^{-1}) (water–acetone): 452 (15200). δ_H (300 MHz, CD_3CN) 9.44 (H12; 2H, d, J = 5.4 Hz), 8.38 (H3′; 2H, s), 8.33 (H3; 2H, s), 8.12 (H10; 2H, d, J = 8.3 Hz), 7.81 (H11, 2H, dd, J = 8.3, 5.4 Hz), 7.63 (H6′; 2H, d, J = 5.4 Hz), 7.41 (H6, 2H, d, J = 5.4 Hz), 7.28 (H5′; 2H, d, J = 5.4 Hz), 7.03 (H5, 2H, d, J = 5.4 Hz), 3.34 (H13a,b; s, 2H), 2.58 (4Me′; s, 6H), 2.46 (4Me; s, 6H), 2.10 (H13a,b; s, 2H). MS (ESMS, CH_3CN, M = 1047.8); m/z = 901.1 $(M - PF_6)^+$. CD: λ/nm ($\Delta\varepsilon$/dm^3 mol^{-1} cm^{-1}) (ethanol–water): Δ isomer: 386 (+50.4); 464 (−45.4); Λ isomer: 386 (−59.9); 464 (+45.9). Optical purity at 464 nm = 98.9%.[39]

$Ru(bpyMe_2)_2(dppz)](PF_6)_2 \cdot 2H_2O$: 85%. λ_{max}/nm (ε/dm^3 mol^{-1} cm^{-1}) (water–acetone): 443 (16300). δ_H (300 MHz, CD_3CN) 9.68 (H12; 2H, d, J = 5.4 Hz), 8.05 (H11, 2H, dd, J = 8.3, 5.4 Hz), 8.72 (H3′; 2H, s), 8.69 (H3; 2H, s), 8.52 (H10; 2H, d, J = 8.3 Hz), 8.47 (H13; 2H, dd, J = 6.0, 6.0 Hz), 8.18 (H14; 2H, dd, J = 6.0, 6.0 Hz), 7.97 (H6′; 2H, d, J = 5.4 Hz), 7.87 (H6, 2H, d, J = 5.4 Hz), 7.46 (H5′; 2H, d, J = 5.4 Hz), 7.22 (H5, 2H, d, J = 5.4 Hz), 2.61 (4Me′; s, 6H), 2.50 (4Me; s, 6H), 2.10 (H13a,b; s, 2H). MS (ESMS, CH_3CN, M = 1043.8); m/z = 897.4 $(M - PF_6)^+$. CD: λ/nm ($\Delta\varepsilon$/dm^3 mol^{-1} cm^{-1}) (ethanol–water): Δ isomer: 390 (+72); 467 (−58.3); Λ isomer: 390 (−77.7); 467 (+56.6). Optical purity at 467 nm = 97.2%.[39]

DNA-paper chromatography

The DNA-paper used for chromatography was prepared as previously reported.[20] DNA paper and untreated chromatographic paper were individually spotted with the desired complex hexafluorophosphate dissolved in the minimum amount of acetone. Multiple samples were spotted (5 μL) on each sheet leaving at least 2 cm between them to avoid cross contamination. The sheets were placed in a chromatography tank containing sodium acetate buffer (0.16 M, pH 6.9) incorporating 10% v/v methanol and eluted. The paper was removed from the tank and allowed to air dry. The leading points of the bands on the paper were then marked from visually observable coloration or with the aid of an UV lamp.

Absorption spectroscopy in the presence of CT-DNA

All absorption spectra were carried out using Tris–HCl buffer (tris(hydroxymethyl)aminomethane hydrochloride (5 mM)–NaCl (50 mM) adjusted to pH 7.5). Complexes were prepared as chloride salts and kept in the dark to avoid decomposition. The ratio of metal complex (20 μM) to DNA base pairs (100 μM) was achieved by the addition of known quantities of CT-DNA determined spectrophotometrically using the molar absorptivity of 13200 M^{-1} cm^{-1} at 258 nm,[33] (100 μM). The concentration of metal complex was also determined spectrophotometrically using extinction coefficients reported in the synthetic method. After mixing, the complex–DNA solutions were allowed to equilibrate for 20 min at 20 °C. Absorbance was corrected using the buffer alone.

DNA viscosity measurements

Viscosity measurements were carried out using a Cannon-Manning semi-micro viscometer maintained at a constant temperature of 25 °C in a water bath. CT DNA, sonicated to approximately 200 base pair lengths was prepared and purified according to the method of Chaires *et al.*[33] The viscometer required 300 μL of sample and the flow time for the BPES buffer (8 mM sodium phosphate–1 mM disodium EDTA–25 mM NaCl, pH 7.0) used in these experiments was 465 ± 2 s. The DNA concentration was 100 μM per base pair (molar absorptivity of 13200 M^{-1} cm^{-1} at 258 nm) and samples were prepared to give total metal complex/base pair ratios of 0.0714, 0.125 and 0.25. Flow times were measured after a thermal equilibration time of 30 min. Each sample was measured five times and from these values an average flow time was calculated. The established intercalator, ethidium bromide, and groove binder, Hoechst 33258, were included as reference points. Viscosity is presented as $(\eta/\eta^0)^{1/3}$ in accordance with the theory of Cohen and Eisenberg.[34]

Submarine gel electrophoresis

Agarose was heated until it had completely melted and was dissolved in TAE buffer (tris(hydroxymethyl)aminomethane (40 mM)–acetic acid (20 mM)–ethylenediaminetraacetic acid (1mM), pH 8.0) to give a final concentration of 1% w/v. Supercoiled pBR322 plasmid DNA from *E. Coli* was incubated in Eppendorf tubes at 37 °C at a final concentration of 40 μM per base pair with the metal complex also at 40 μM. Loading buffer was also present to help the mixtures sink into the wells on the gel and to visualise the progress of the bands. Electrophoresis was carried out for 1 h at 100 V to separate the covalently closed circular DNA (Type I), the nicked open circular form (Type II) and the linear form (Type III) as well as any topoisomers present. The gels were removed from the horizontal electrophoresis apparatus and immersed for 10 min in ethidium bromide solution (0.5 mg cm^{-3}), which fluoresces strongly when bound to DNA. The gel was then washed in water for a further 10 min. Visualisation of the dye and thus the DNA was achieved by placing the gel on a transilluminator and photographing.

Results and discussion

Synthesis

The syntheses of the ligands dpq, dpqc and dppz from 1,10-phenanthroline-5,6-dione were straightforward condensations of carbonyl and amine groups that auto-oxidise to the resulting phenazine ring systems. The complexation of the intercalative ligands with the neutral *cis*-$[Ru(bpyMe_2)_2Cl_2]$ complex to produce the desired mixed ligand tris-bidentate octahedral Ru(II) complexes, gave relatively high yields and the formation of a deep red colour was a good indication of the reaction progress. The hexafluorophosphate salts of all complexes were extremely insoluble in water. Slow addition of the sodium hexafluorophosphate allowed the formation of a precipitate that could be successfully filtered. Recrystallisation of the complexes from acetone and water was not always successful so the remaining crude compounds were chromatographed on neutral aluminium oxide in acetonitrile, collecting the major deep red bands, discarding the leading and trailing portions.

Fig. 1 shows the structures and proton numbering of the complexes using $[Ru(bpyMe_2)_2(dpqc)](PF_6)_2$ as an example. The resonances of each metal complex were assigned with the aid of the previously reported spectra of related compounds[1–3,9–11,15,17–18,35] and the COSY spectrum for $[Ru(bpyMe_2)_2(dpqc)]^{2+}$.

The assignment of the absolute configurations of the resolved complexes in this study is based on CD analyses and comparison with similar complexes whose absolute configuration has been determined by X-ray crystallography. In accordance with the assignments by Bosnich[40,41] for similar Ru(II)–polypyridyl complexes, all enantiomers having positive CD maxima at 450 nm and negative CD maxima at 310 nm were assigned as Δ whereas enantiomers having the opposite sign at the same wavelengths were assigned the Λ-configuration. In this work, enantiomeric purity was judged to be 100% for the enantiomer with the highest Cotton effect and in most cases the enantiomers were within 5% of each other.

Table 1 DNA paper chromatographic results

Metal complex	Band distance (blank)/cm	Solvent front (blank)/cm	R_f (blank)	Band distance (DNA)/cm	Solvent front (DNA)/cm	R_f (DNA)	ΔR_f
Δ-[Ru(bpyMe$_2$)$_2$(phen)]$^{2+}$	19.0	23.0	0.83	15.6	24.0	0.65	0.18
rac-[Ru(bpyMe$_2$)$_2$(phen)]$^{2+}$	18.4	23.0	0.80	16.3	23.8	0.68	0.12
Λ-[Ru(bpyMe$_2$)$_2$(phen)]$^{2+}$	20.0	23.1	0.87	14.4	24.2	0.60	0.27
Δ-[Ru(bpyMe$_2$)$_2$(dpq)]$^{2+}$	12.9	19.1	0.68	4.2	15.1	0.28	0.40
rac-[Ru(bpyMe$_2$)$_2$(dpq)]$^{2+}$	14.0	19.6	0.71	5.4	14.9	0.36	0.35
Λ-[Ru(bpyMe$_2$)$_2$(dpq)]$^{2+}$	14.0	19.8	0.71	5.0	14.0	0.36	0.35
Δ-[Ru(bpyMe$_2$)$_2$(dpqc)]$^{2+}$	12.2	23.5	0.52	1.9	22.8	0.08	0.44
rac-[Ru(bpyMe$_2$)$_2$(dpqc)]$^{2+}$	8.1	23.2	0.35	3.2	22.5	0.14	0.21
Λ-[Ru(bpyMe$_2$)$_2$(dpqc)]$^{2+}$	11.9	23.0	0.52	4.5	21.8	0.21	0.31
Δ-[Ru(bpyMe$_2$)$_2$(dppz)]$^{2+}$	8.5	23.6	0.36	2.2	24.7	0.09	0.27
rac-[Ru(bpyMe$_2$)$_2$(dppz)]$^{2+}$	6.7	23.7	0.28	2.2	24.2	0.09	0.19
Λ-[Ru(bpyMe$_2$)$_2$(dppz)]$^{2+}$	9.8	23.6	0.42	2.2	24.0	0.09	0.33

DNA paper chromatography

DNA paper chromatography has shown itself to be a reliable and straightforward means of determining the relative affinity of a compound for nucleic acids. While the nature of this particular test renders it incapable of differentiating between the various reversible interactions that molecules can have with DNA, nevertheless, it has demonstrated the enantioselectivity of DNA and raised questions about the combined effects of enantiomers as opposed to the interactions they have by themselves.

Due to the way DNA paper dries, inconsistencies in the paper's surface give rise to areas where solvent travels at different rates. This phenomenon leads to an uneven solvent front, and therefore requires that individual solvent retentions are calculated for each lane on the paper. This is indicative of the low resolution of such a chromatographic system, but obvious and expected trends across the Ru(II)–polypyridyl series were observed (Fig. 2). Table 1 details the retention data for the metal

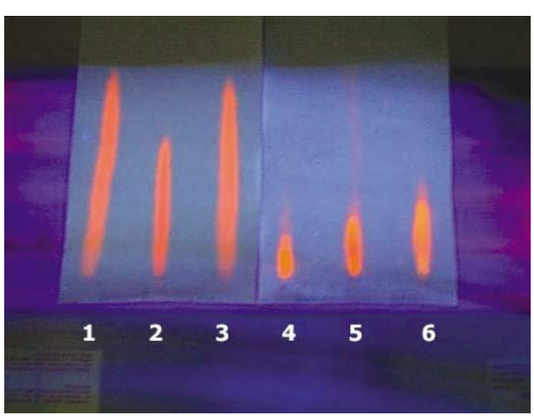

Fig. 2 Effects of Δ,Λ-[Ru(bpyMe$_2$)$_2$(dpqc)]$^{2+}$ on DNA paper chromatography. Lanes 1, 2 and 3 correspond to the Δ-, *rac*- and Λ-isomers on blank cellulose chromatography paper, while lanes 4, 5 and 6 are the same isomers on the DNA treated paper. Samples were eluted by a sodium acetate buffer (0.16 M, pH 6.9, 10% methanol). The lanes were photographed under UV illumination.

complexes on the DNA paper and the untreated paper, which is illustrated in Fig. 3. From this data, there is a clear pattern relating an increased affinity signified by the lower distances travelled, to larger intercalating ligands present in the complex. Moreover, the trend in affinity for the Δ- and Λ-isomers corroborate earlier observations.[19] Δ-[Ru(bpyMe$_2$)$_2$(dpq)] and Δ-[Ru(bpyMe$_2$)$_2$(dpqc)] had lower R_f values (higher affinity) than their mirror images. In contrast, Λ-[Ru(bpyMe$_2$)$_2$(phen)] has a higher affinity than the Δ-isomer in keeping with reported binding affinities of 1.1×10^4 and 0.9×10^4, respectively.[14]

Absorption spectroscopy

The absorption spectra of Ru(II)–polypyridyl complexes are

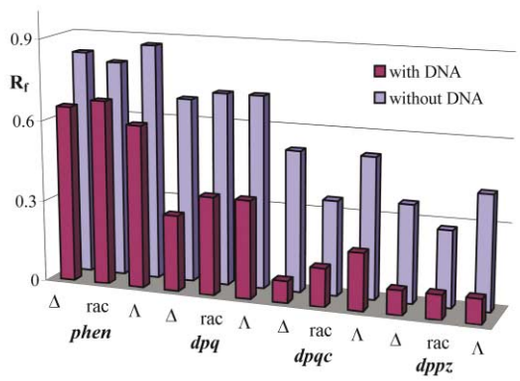

Fig. 3 Bar graph showing the relative distances travelled by the [Ru(bpyMe$_2$)$_2$L]$^{2+}$ series (where L = phen, dpq, dpqc and dppz) on DNA paper and untreated cellulose chromatographic paper. Retention factors were determined with respect to sodium acetate buffer (0.16 M, pH 6.9, 10% methanol) solvent front.

sensitive to changes in their environment and are thus able to give an indication of their association with nucleic acids. The analysis is mainly concerned with the visible region where the complexes, but not the DNA, absorb. The visible absorption is a result of electronic transitions of the MLCT band and these transitions are changed when the chromophore is closely associated with another molecule or group.

All of the complexes studied by absorption spectroscopy, except for Λ-[Ru(bpyMe$_2$)$_2$(phen)]$^{2+}$, showed visible hypochromism at their absorption maxima, as can be seen in Table 2. Bathochromic or red shifting in the 490 nm region of the absorption band was observed for all complexes except Δ-[Ru(bpyMe$_2$)$_2$(dppz)]$^{2+}$ and for Δ-[Ru(bpyMe$_2$)$_2$(phen)]$^{2+}$ for which insignificant 1 nm shifts were observed. As the combination of the hypochromism and bathochromism is believed to be indicative of intercalation,[25] these results seem puzzling. For Δ-[Ru(bpyMe$_2$)$_2$(dppz)]$^{2+}$ the lack of any red shift at this region was unexpected, although it did show a significant hypochromic shift (3.4%). The combination of these results do not negate the possibility that Δ-[Ru(bpyMe$_2$)$_2$(dppz)]$^{2+}$ is an intercalator, as the near UV intra-ligand (IL) band shows a significant hypochromic shift (33.4%) and slight red shift (2 nm) similar to the other dppz complexes indicative of intercalation.

Submarine gel electrophoresis

The unwinding of supercoiled pBR322 plasmid DNA in the presence of Ru(II)–polypyridyl complexes has been monitored by migration patterns through agarose gel based electrophoretic techniques. Intercalators need to unwind supercoiled DNA in order for them to bind, and the more unwinding that occurs in a given sample of plasmid DNA, the larger and thus slower its migration rate is through the gel. Unwinding of the supercoiled pBR322 plasmid was observed at the metal complex concentrations used.

Table 2 Spectroscopic properties concerning the MLCT bands of selected Ru(II)–polypyridyl complexes on binding to DNA

Complex	Absorption maxima			Red shift at 490 nm	Hypochromic shift (%)	Isosbestic point/nm
	Free	Bound	$\Delta\lambda$/nm			
Δ-[Ru(bpyMe$_2$)$_2$(phen)]$^{2+}$	454	454	0	1	1.0	—
Λ-[Ru(bpyMe$_2$)$_2$(phen)]$^{2+}$	454	454	0	0	0.2	—
Δ-[Ru(bpyMe$_2$)$_2$(dpq)]$^{2+}$	443	441	−2	4	1.7	479
Λ-[Ru(bpyMe$_2$)$_2$(dpq)]$^{2+}$	443	442	−1	4	2.0	475
Δ-[Ru(bpyMe$_2$)$_2$(dpqc)]$^{2+}$	452	456	4	3	4.0	474
Λ-[Ru(bpyMe$_2$)$_2$(dpqc)]$^{2+}$	452	445	−7	5	8.2	475
Δ-[Ru(bpyMe$_2$)$_2$(dppz)]$^{2+}$	442	444	2	0	3.4	498
Λ-[Ru(bpyMe$_2$)$_2$(dppz)]$^{2+}$	442	445	3	4	5.3	479

For the complex [Ru(bpyMe$_2$)$_2$(phen)]$^{2+}$, there were no observable differences in the migration pattern and that of the untreated DNA, which suggests that it did not unwind plasmid DNA to any degree at all even at a high metal loading concentration (Fig. 4, lanes 5, 6 and 7 represent Δ-, *rac*- and Λ-[Ru-

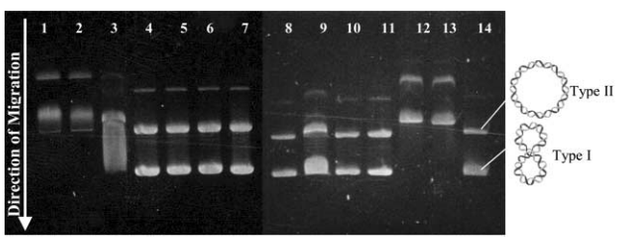

Fig. 4 Unwinding effects of the metal complexes on 1% agarose (with ethidium bromide) of *E. Coli* pBR322 Plasmid DNA. The smear represents a gradient of several topoisomers of slightly varying overall size. Lanes 1, 2 and 3 represent Δ-, *rac*- and Λ-[Ru(bpyMe$_2$)$_2$(dppz)]$^{2+}$, lanes 5, 6 and 7 represent Δ-, *rac*- and Λ-[Ru(bpyMe$_2$)$_2$(phen)]$^{2+}$, lanes 8, 9 and 10 represent Δ-, *rac*- and Λ-[Ru(bpyMe$_2$)$_2$(dpq)]$^{2+}$ and lanes 12, 13 and 14 represent Δ-, *rac*- and Λ-[Ru(bpyMe$_2$)$_2$(dpqc)]$^{2+}$, respectively. Lanes 4 and 11 are untreated DNA control.

(bpyMe$_2$)$_2$(phen)]$^{2+}$). This result indicates that neither Δ, or Λ-[Ru(bpyMe$_2$)$_2$(phen)]$^{2+}$ intercalate to any extent. In recent articles Λ-[Ru(phen)$_3$]$^{2+}$ has been reported as a partial intercalator[21] it would seem that replacement of the phen with bpyMe$_2$ stops insertion all together. The result obtained for the [Ru(bpyMe$_2$)$_2$(dppz)]$^{2+}$, is in stark contrast to those of the phen complexes (Fig. 4, lanes 1, 2 and 3 represent Δ, *rac*- and Λ-[Ru(bpyMe$_2$)$_2$(dppz)]$^{2+}$). Δ- and *rac*- samples significantly slowed the migration while the Λ-enantiomer caused an even smearing effect of the nicked DNA between the regions corresponding to the control DNA. This set of results are significant in that they show that the dppz moiety is highly capable of intercalating when complexed, hence the marked unwinding of the plasmid. The Λ isomer does not bind as selectively and so does not fully unwind the plasmid. The incorporation of bpyMe$_2$ as the non-intercalative peripheral ligands has successfully brought about an enantioselective response with the DNA. The smearing effect observed for the Λ-isomer is also indicative of helical unwinding albeit to a less efficient extent than that of the Δ-isomer. The smear represents a gradient of several topoisomers of slightly varying overall size. The conclusions that can be drawn from this is that the extended methyl groups in the 4 and 4′-positions on the bpyMe$_2$ ligand are critical in eliciting different steric interactions with the walls of the DNA grooves. In the case of the Δ-isomer of [Ru(bpyMe$_2$)$_2$-(dppz)]$^{2+}$ the intercalator keeps the peripheral ligands away from the DNA groove walls and thus cause unwinding, but the unfavourable steric interactions these methyl groups have with the groove walls give rise to less efficient intercalation for the Λ-isomer. This species is still intercalating nevertheless, but there is less intercalation overall in the plasmid, and this most probably arises due from the fact that there is much variation of the DNA properties in the native supercoiled plasmid, with many sites being more accessible and potentially reactive than others. An important consideration is the fact that the *rac*- sample showed identical activity to the Δ-isomer and not an average of the Δ- and Λ-enantiomers. The reason for this phenomenon is because the amount of Δ-enantiomer in the *rac*-sample was more than enough to interact with the maximum available sites.

rac-[Ru(bpyMe$_2$)$_2$(dpq)]$^{2+}$ showed correspondingly higher levels of unwinding than the enantiomers by themselves. The Δ- and Λ-isomers of [Ru(bpyMe$_2$)$_2$(dpq)]$^{2+}$ showed practically no activity at all whereas the *rac*- sample showed significant smearing of the nicked and circular DNAs (Fig. 4, lanes 8, 9 and 10 represent Δ-, *rac*- and Λ-[Ru(bpyMe$_2$)$_2$(dpq)]$^{2+}$). These results point toward a synergistic effect between the enantiomers for unwinding plasmid DNA although exactly how this is accomplished is not understood. Stacking of planar aromatic moieties has been documented for similar metal complex systems,[42,43] so it may be possible that the mirror image isomers associate in a way that two of the same isomer cannot and hence lead to effects that are different from the individual components.

The dpqc ligand is practically the same size as the dppz ligand, the only difference being that the endmost ring is aliphatic and its potential for intercalation is expected to be somewhere in between that of dpq and dppz, and the electrophoretic results obtained in this study are in agreement with these assumptions. Showing some similarities to the dppz complexes, nearly all of the dpqc containing complexes slowed the progress of the plasmid DNA through the gel. For the [Ru-(bpyMe$_2$)$_2$(dpqc)]$^{2+}$ complexes a similar phenomenon to that of the [Ru(bpyMe$_2$)$_2$(dppz)]$^{2+}$ occurred as the Δ- and *rac*- samples caused maximum unwinding whereas the Λ-isomer caused no unwinding at all (Fig. 4, lanes 12, 13 and 14 represent Δ-, *rac*- and Λ-[Ru(bpyMe$_2$)$_2$(dpqc)]$^{2+}$) . Again it is the unfavourable steric interactions between the bpyMe$_2$ ligands and the DNA groove walls that elicit this enantioselectivity, as was the case for [Ru(bpyMe$_2$)$_2$(dppz)]$^{2+}$. The major difference is that the driving force of the complexed dppz was strong enough to still afford intercalation.

Viscosity studies of rodlike DNA

The resolved enantiomers of the [Ru(bpyMe$_2$)$_2$L]$^{2+}$ series were tested for their effects on sonicated 200 base pair length rods of DNA. Different concentrations of metal complex were tested in the presence of the 100 μM bp DNA to give final mixing ratios of 0.042, 0.125 and 0.250. The results obtained from the viscometric analysis were most enlightening in terms of being able to discriminate between the various binding modes. The established intercalator ethidium bromide and groove binder Hoechst 33258 were included as reference compounds. Both behaved as expected, as can be seen in Fig. 5. Ethidium increased the relative specific viscosity of the DNA in a linear fashion until a ratio *r* of approximately 0.1 drug/DNA base pair was reached, where the slope began to decrease, indicating the further lengthening of the DNA as more drug was added. The groove binder Hoechst 33258 showed no significant effect on the DNA regardless of the mixing ratio. As for the metal

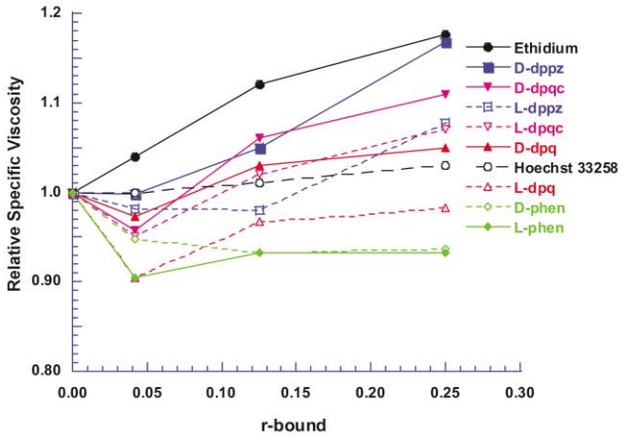

Fig. 5 Effects of increasing amounts of Δ,Λ-$[Ru(bpyMe_2)_2(phen)]^{2+}$(◆, ◇); Δ,Λ-$[Ru(bpyMe_2)_2(dpq)]^{2+}$ (▲, Δ); Δ,Λ-$[Ru(bpyMe_2)_2(dpqc)]^{2+}$ (▼, ▽) and Δ,Λ-$[Ru(bpyMe_2)_2(dppz)]^{2+}$ (■, □); on the specific relative viscosity of 200 Bp linear CT-DNA. Viscosity is presented as $(\eta/\eta^0)^{1/3}$ in accordance with the theory of Cohen and Eisenberg.[36] The established intercalator ethidium (●) and proven groove binder Hoechst 33258 (○) are shown for reference. The total ligand to base pair ratios measured were 0.0417, 0.125 and 0.25.

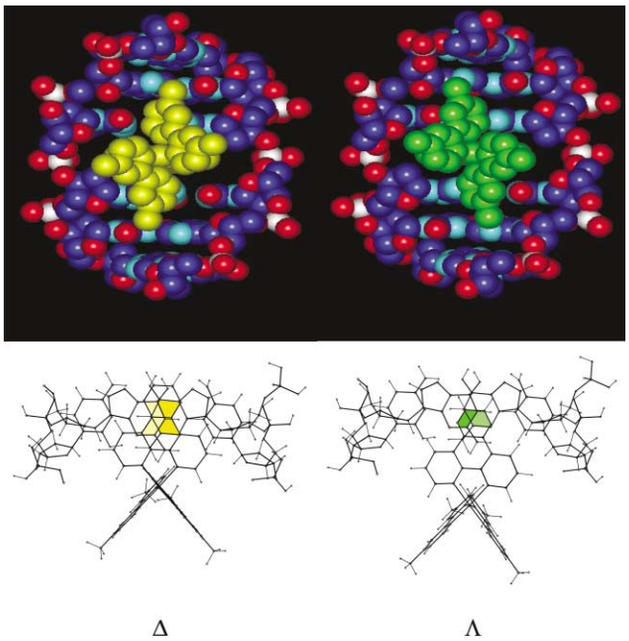

Fig. 6 Δ- and Λ-$[Ru(bpyMe_2)_2(dpq)]^{2+}$ and their associations with helical DNA. The above space-filling representation shows the favoured fit of the peripheral $bpyMe_2$ ligands of the Δ-enantiomer with the groove of the DNA. The poorer modelled fit of the Λ-isomer translates to the inability of the molecule to insert its dpq ligand far enough into the base pair stack and thus fully intercalate. The bottom wireframe representation shows the proposed aromatic overlap (shaded) that the dpq ligand can afford with the aromatic bases of the DNA for each enantiomer.

complexes there was a broad range of effects ranging from significant lengthening similar to that of ethidium, to DNA shortening analogous to the partial intercalating originally described for the aromatic diammonium cations tested by Kapicak and Gabbay.[44]

The Δ-isomer of $[Ru(bpyMe_2)_2(dppz)]^{2+}$ brought about the greatest lengthening of the DNA, with a relative specific viscosity of 1.17 at $r = 0.250$ drug/base pair ratio, practically as high as for ethidium, and this result alone signifies that metallo-intercalators can be just as effective as their classical organic counterparts. The next most effective species was the Δ-isomer of $[Ru(bpyMe_2)_2(dpqc)]^{2+}$ which yielded a value of 1.11 for the same ratio ($r = 0.250$). The Δ-$[Ru(bpyMe_2)_2(dpqc)]^{2+}$ isomer increased the viscosity more than the Λ-$[Ru(bpyMe_2)_2(dppz)]^{2+}$. The Δ-isomers of all the complexes exhibit higher viscosity than their enantiomers, and this same trend was encountered in the viscometric testing of the similar Ru(II) complex $[Ru(phen)_2(dppz)]^{2+}$.[14]

$[Ru(bpyMe_2)_2(dpq)]^{2+}$ proved to be a very interesting species as the Δ-isomer increased the viscosity of the DNA solution, while the Λ-enantiomer actually decreased it, signifying that the enantiomers bind through different modes. This stereochemical discrimination points toward the dpq ligand affording weak intercalation when coordinated to a Ru(II) system with extended peripheral ligands. The orientation of the peripheral $bpyMe_2$ ligands influences how far the intercalator can insert into the base pair stack, as illustrated in Fig. 6, where the dpq ligand of the Δ-isomer can fully insert while the Λ-isomer can only partial intercalate. The incorporation of $bpyMe_2$ as a peripheral ligand in this study was expected to provide some details on the effects of steric interactions between the non-intercalated ligands and the walls of the DNA grooves. From the results it appears that the methyl groups in the 4 and 4′ positions protrude into the groove walls and restrict the Λ-complex from fully intercalating. Viscometric analysis of the enantiomers of the similar complex $[Ru(phen)_2(dpq)]^{2+}$ failed to demonstrate this phenomenon, as both the Δ- and Λ-isomers were capable of classically intercalating.[10] Whereas viscosity measurements of the complex $[Ru(2,9\text{-}phen)_2(dpq)]^{2+}$ showed an increase in the relative viscosity of the DNA upon addition of the Δ-enantiomer, a decrease in the relative viscosity of the DNA was observed upon addition of the Λ-metal complex. Futhermore, DNA-NMR binding studies suggested that the dpq ligand of the Δ-enantiomer intercalated deeply into the hexanucleotide base stack while the Λ-enantiomer could only partially intercalate as a consequence of the position of the methyls.[11]

Along with Λ-$[Ru(bpyMe_2)_2(dpq)]^{2+}$, both optical hands of $[Ru(bpyMe_2)_2(phen)]^{2+}$ reduced the length of the rod-like DNA, albeit to a higher degree. These results indicate that the methyl groups on the $bpyMe_2$ ligands simply do not allow the phen ligand to penetrate far enough into the base pair stack to cause DNA to unwind, so lengthening is not observed. This model seems to fit nicely with the results obtained by Satyanarayana *et al.*[5] who found through similar viscometric analysis that neither of the enantiomers of $[Ru(phen)_3]^{2+}$ could classically intercalate into DNA. Their results suggested that the Δ-enantiomer would partially intercalate, and the Λ-enantiomer fails to significantly alter the length of DNA, implying groove binding or perhaps simpler electrostatic associations, such as that proposed for $[Ru(bpy)_3]^{2+}$.[45]

As most of the viscometric analysis has focussed on the highest drug/DNA ratio, what has not been covered is the inconsistent variations in DNA length. Over the range analysed, many compounds overlap and often start off by decreasing the persistent length and then as the ratios increase, start to lengthen the polymer, as can be seen in Fig. 5. To explain this behaviour it is important to remember that DNA–drug interactions are subject to equilibria with multiple binding sites of varying reactivity. It is quite possible that these allosteric considerations play an important part in these associations and the fact that the reactions are reversible could only contribute to inconsistent results of this type. As the length of the nucleic acid is under scrutiny here, and having established the individual effects that classical and partial intercalation have on it, an important factor to consider is the final amount of binding of the drug to the DNA. In terms of classical intercalation, the more drugs bound will simply give rise to a longer length of DNA, but as partial intercalation induces static bends, it has the potential to change DNA in three dimensions.[46] What this means is that for a given length of DNA, equivalent numbers of

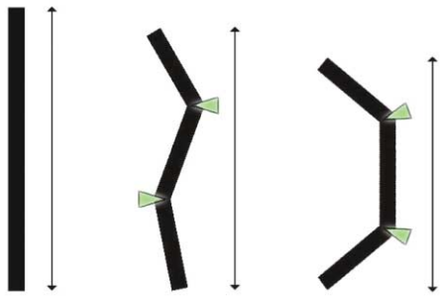

Fig. 7 Two-dimensional schematic representing the decrease in helical length as a result of partial intercalation. The structure on the left represents a native length of double helical DNA. The structure in the middle represents the same length of DNA with two partially intercalating species bound in an alternating consecutive fashion. The structure on the right is the same length of DNA but with two consecutive partial intercalators bound from the same side. Note the different lengths achieved by an equivalent number of partially intercalating species depending on the position and side of the DNA in which they bind.

bound species can give rise to differing lengths depending on the specific sites that they occupy (Fig. 7). As DNA is a spiralling double helix, the bound substrates can insert towards the DNA axis from practically any angle with respect to each other. In theory this means that for a sample of rodlike DNA with partially intercalated species bound at various sites, a viscometric average of all the possible combinations of drug–DNA lengths is represented in the results. This effect was clearly illustrated in recent work by Hannon *et al.*[47] where the end-to-end length of of linearised pBR322 was dramatically reduced upon the addition of $[Ru(phen)_3]^{2+}$. The AFM images clearly shows that the once linear DNA has been bent several times forming compact semi-cirles and U-shapes.

No efforts were made to relate the actual lengths of the DNA drug duplex to the relative viscosity values obtained. However, in light of this possibility, an accurate model of multiple partial intercalation would be difficult to achieve, especially when no information about the angles of these static bends is known. Partial intercalation would account for the shortening of DNA at the lower drug/base pair ratios, however as the ratio increased and more drug bound, the DNA would then be lengthened until saturation was reached. For both enantiomers of $[Ru(bpyMe_2)_2(phen)]^{2+}$ and Λ-$[Ru(bpyMe_2)_2(dpq)]^{2+}$, this saturation appears to be reached at ratio $r = 0.125$. Another important factor to consider is that the partial intercalation cannot be quantified in this relationship, unlike classical intercalation, which relates the amount of bound drug to the persistent length of the nucleic acid.

Conclusion

The techniques employed here were successful in elucidating the relative binding affinities and binding modes of the metal complexes investigated. Corroborative results were obtained across the various techniques and highlighted trends within the series of complexes. DNA paper chromatography confirmed that the size of the intercalating ligand influences the binding affinity in the order of phen < dpq < dpqc < dppz and, in the majority of the cases, the Δ-isomer exhibited a stronger affinity for DNA. Absorption spectroscopy experiments strengthen the opinion that dpq, dpqc and dppz are closely associated with DNA while electrophoresis experiments identified differences between binding efficiency of the enantiomers of $[Ru(bpyMe_2)_2(dpqc)]^{2+}$ and $[Ru(bpyMe_2)_2(dppz)]^{2+}$. Viscosity measurements were able to determine that $bpyMe_2$ modulates the binding interactions so that Δ-$[Ru(bpyMe_2)_2(dpq)]^{2+}$ binds by intercalation whereas Λ-$[Ru(bpyMe_2)_2(dpq)]^{2+}$ insertion is restricted and it can only partially intercalate. An example of enantiomeric discrimination was observed for the $[Ru(bpyMe_2)_2L]^{2+}$ series, in particular Δ and Λ-$[Ru(bpyMe_2)_2(dpq)]^{2+}$ indicating the importance of the choice of peripheral ligand and its overall effect on binding.

Acknowledgements

The support of the Australian Research Council and the University of Western Sydney, Macarthur are gratefully acknowledged. We also wish to thank Macquarie University for the use of their circular dichroism spectrometer.

References and notes

1 J. K. Barton, A. T. Danishefsky and J. M. Goldberg, *J. Am. Chem. Soc.*, 1984, **106**, 2172.
2 J. K. Barton, J. M. Goldberg, C. V. Kumar and N. J. Turro, *J. Am. Chem. Soc.*, 1986, **108**, 2018.
3 C. Hiort, B. Nordén and A. Rodger, *J. Am. Chem. Soc.*, 1990, **112**, 1971.
4 J. M. Kelly, A. B. Tossi, D. J. McConnell and C. OhUigin, *Nucleic Acids Res.*, 1985, **13**, 6017.
5 S. Satyanarayana, J. C. Dabrowiak and J. B. Chaires, *Biochemistry*, 1992, **31**, 9319.
6 M. Eriksson, M. Leijon, C. Hiort, B. Nordén and A. Gräslund, *Biochemistry*, 1994, **33**, 5031.
7 J. P. Rehman and J. K. Barton, *Biochemistry*, 1990, **29**, 1701.
8 J. P. Rehman and J. K. Barton, *Biochemistry*, 1990, **29**, 1710.
9 I. D. Greguric, J. R. Aldrich-Wright and J. G. Collins, *J. Am. Chem. Soc.*, 1997, **119**, 3621.
10 J. G. Collins, A. D. Sleeman, J. R. Aldrich-Wright, I. Greguric and T. W. Hambley, *Inorg. Chem.*, 1998, **37**, 2133.
11 J. G. Collins, J. R. Aldrich-Wright, I. D. Greguric and P. A. Pellegrini, *Inorg. Chem.*, 1999, **38**, 3502.
12 C. Hiort, P. Lincoln and B. Nordén, *J. Am. Chem. Soc.*, 1993, **115**, 3448.
13 R. E. Holmlin, E. D. A Stemp and J. K. Barton, *J. Am. Chem. Soc.*, 1994, **116**, 9840.
14 I. Haq, P. Lincoln, D. Suh, B. Nordén, B. Z. Chowhry and J. B. Chaires, *J. Am. Chem. Soc.*, 1995, **117**, 4788.
15 A. Greguric, I. D. Greguric, T. W. Hambley, J. R. Aldrich-Wright and J. G. Collins, *J. Chem. Soc., Dalton Trans.*, 2002, 849.
16 J. E. Dickeson and L. A. Summers, *Aust. J. Chem.*, 1970, **23**, 1023.
17 J. R. Aldrich-Wright, PhD Thesis, Macquarie University, 1993.
18 I. D. Greguric, PhD Thesis, University of Western Sydney, 1999.
19 J. K. Barton, L. A. Basile, A. Danishefsky and A. Alexandrescu, *Proc. Natl. Acad. Sci. USA*, 1984, **81**, 1961.
20 J. R. Aldrich-Wright, I. Greguric, R. S. Vagg, K. Vickery and P. A. Williams, *J. Chromatogr. A*, 1995, **718**, 436.
21 D. Z. Coogan, I. S. Haworth, P. J. Bates, A. Robinson and A. Rodger, *Inorg. Chem.*, 1999, **38**, 4486.
22 I. S. Haworth, A. H. Elcock, J. Freeman, A. Rodger and W. G. Richards, *J. Biomol. Struct. Dyn.*, 1991, **9**, 23.
23 I. S. Haworth, A. H. Elcock, A. Rodger and W. G. Richards, *J. Biomol. Struct. Dyn.*, 1991, **9**, 553.
24 S. A. Tysoe, A. D. Baker and T. C. Strekas, *J. Phys. Chem.*, 1993, **97**, 1707.
25 J-P. Lecomte, A. Kirsch-De Mesmaeker, M. M. Feeney and J. M. Kelly, *Inorg. Chem.*, 1995, **34**, 6481.
26 W. Keller, *Proc. Natl. Acad. Sci. USA*, 1975, **72**, 4876.
27 A. M. Pyle, J. P. Rehmann, R. Meshoyrer, C. V. Kumar, N. J. Turro and J. K. Barton, *J. Am. Chem. Soc.*, 1989, **111**, 3051.
28 M. J. Waring, *J. Mol. Biol.*, 1970, **54**, 247.
29 A. B. Tossi and J. M. Kelly, *Photochem. Photobiol.*, 1989, **49**, 545.
30 A. Aboul Enein and D. Schulte-Frohlinde, *Photochem. Photobiol.*, 1988, **48**, 27.
31 L. S. Lerman, *J. Mol. Biol.*, 1961, **3**, 18.
32 D. Suh and J. B. Chaires, *Bioinorg. Med. Chem.*, 1995, **3**(6), 723.
33 J. B. Chaires, N. Dattagupta and D. M. Crothers, *Biochemistry*, 1982, **21**, 3933.
34 G. Cohen and H. Eisenberg, *Biopolymers*, 1969, **8**, 45.
35 M. Yamada, Y. Tanaka, Y. Yoshimoto, S. Kuroda and I. Shimao, *Bull. Chem. Soc. Jpn.*, 1992, **65**, 1006.
36 B. P. Sullivan, D. J. Salmon and T. J. Meyer, *Inorg. Chem.*, 1978, **12**, 3334.
37 T. J. Rutherford, P. A. Pellegrini, J. R. Aldrich-Wright, P. C. Junk and F. R. Keene, *Eur. J. Inorg. Chem.*, 1998, 1677.

38 E. D. Seddon, K. J. Seddon, *The Chemistry of Ruthenium*, Elsevier, Amsterdam, 1984, p. 1173.
39 Optical purity = [−((Λ) $\Delta\varepsilon^{max}$/(Δ) $\Delta\varepsilon^{max}$)]. Note: to keep the numerical figure less than one, the largest $\Delta\varepsilon^{max}$ from either the Λ or Δ isomer was placed as the numerator when divided: $\Delta\varepsilon$ unit = dm^2 mol^{-1}.
40 B. Bosnich, *Inorg. Chem.*, 1968, **7**, 2379.
41 B. Bosnich, *Inorg. Chem.*, 1968, **7**, 179.
42 N. Gupta, N. Grover, G. A. Neyhart, W. Liang, P. Singh and H. Thorp, *Angew. Chem., Int. Ed. Engl.*, 1992, **31**, 1048.
43 D. Gut, A. Rudi, J. Kopilov, I. Goldberg and M. Kol, *J. Am. Chem. Soc.*, 2002, **124**, 5449.
44 L. Kapicak and E. J. Gabbay, *J. Am. Chem. Soc.*, 1975, **97**, 403.
45 N. J. Turro, J. K. Barton and D. A. Tomalia, *Acc. Chem. Res.*, 1991, **24**, 332.
46 E. Jin, V. Katritch, W. K. Olson, M. Kharatisvili, R. Abagyan and D. S. Pilch, *J. Mol. Biol.*, 2000, **298**, 95.
47 M. J. Hannon, V. Moreno, M. J. Proeto, E. Moldrheim, E. Sletten, I. Meistermann, C. J. Issac, K. J. Sanders and A. Rodger, *Angew, Chem., Int. Ed.*, 2001, **40**, 880.